Published online 16 August 2012 *Nucleic Acids Research, 2012, Vol. 40, No. 19* ***9571–9583***
doi:10.1093/nar/gks755

Genome-wide identification of genes directly regulated by the pleiotropic transcription factor Spx in *Bacillus subtilis*

Tatiana Rochat[1,2], Pierre Nicolas[3], Olivier Delumeau[1,2], Alžbeta Rabatinová[4], Jana Korelusová[4], Aurélie Leduc[3], Philippe Bessières[3], Etienne Dervyn[1,2], Libor Krásný[4] and Philippe Noirot[1,2,*]

[1]INRA, UMR 1319 Micalis, [2]AgroParisTech, UMR Micalis, [3]INRA, UR1077, Mathématique Informatique et Génome, Jouy-en-Josas F-78350, France and [4]Laboratory of Molecular Genetics of Bacteria, Institute of Microbiology, Academy of Sciences of the Czech Republic, Videnska 1083, 142 20 Prague 4, Czech Republic

Received January 18, 2012; Revised July 13, 2012; Accepted July 17, 2012

ABSTRACT

The transcriptional regulator Spx plays a key role in maintaining the redox homeostasis of *Bacillus subtilis* cells exposed to disulfide stress. Defects in Spx were previously shown to lead to differential expression of numerous genes but direct and indirect regulatory effects could not be distinguished. Here we identified 283 discrete chromosomal sites potentially bound by the Spx–RNA polymerase (Spx–RNAP) complex using chromatin immunoprecipitation of Spx. Three quarters of these sites were located near Sigma(A)-dependent promoters, and upon diamide treatment, the fraction of the Spx–RNAP complex increased in parallel with the number and occupancy of DNA sites. Correlation of Spx–RNAP-binding sites with gene differential expression in wild-type and *Δspx* strains exposed or not to diamide revealed that 144 transcription units comprising 275 genes were potentially under direct Spx regulation. Spx-controlled promoters exhibited an extended −35 box in which nucleotide composition at the −43/−44 positions strongly correlated with observed activation. *In vitro* transcription confirmed activation by oxidized Spx of seven newly identified promoters, of which one was also activated by reduced Spx. Our study globally characterized the Spx regulatory network, revealing its role in the basal expression of some genes and its complex interplay with other stress responses.

INTRODUCTION

The bacterial cytoplasm is a highly reducing environment. Upon cell exposure to oxidative stress, disulfide bonds form leading to misfolding and inactivation of proteins. Cells use high concentrations of low-molecular-weight thiol buffers to maintain redox homeostasis, and a variety of reductive enzymatic pathways to remove disulfide bonds. In *Bacillus subtilis*, the thioredoxin pathway is essential for viability (1–3). The expression of the thioredoxin (*trxA*) and thioredoxin reductase (*trxB*) genes is strongly enhanced by the global transcription regulator Spx under disulfide stress (4). The involvement of Spx-like transcriptional regulators in stress responses and/or expression of virulence factors has been reported in several Gram-positive bacteria (5–9). Several *spx*-like genes can be present in one genome where they contribute to the adaptive responses to various stresses. For example, the Spx-like *B. subtilis* MgsR protein modulates a part of the σ^B-mediated global transcriptional response under ethanol stress (10).

The Spx-like proteins form a subfamily within the ArsC (arsenate reductase) family which is structurally different from other transcription factors (TFs) due to the lack of a conserved DNA-binding domain. Spx-mediated regulation is achieved by a direct contact with the C-terminal domain of the RNA polymerase α subunit (RNAP αCTD), allowing either positive or negative transcriptional regulation of genes (4), and no direct contact between Spx and DNA was detected (11). In *B. subtilis*, the activity of Spx is controlled by multiple mechanisms. First, *spx* transcription is negatively regulated by the PerR and YodB repressors and is positively regulated by several

*To whom correspondence should be addressed. Tel: +33 1 34 65 25 14; Fax: +33 1 34 65 25 21; Email: philippe.noirot@jouy.inra.fr
Present address:
Tatiana Rochat, Institut de Génétique et Microbiologie, CNRS, UMR 8621, IFR115, Université Paris-Sud, Orsay, France.

© The Author(s) 2012. Published by Oxford University Press.
This is an Open Access article distributed under the terms of the Creative Commons Attribution Non-Commercial License (http://creativecommons.org/licenses/by-nc/3.0), which permits unrestricted non-commercial use, distribution, and reproduction in any medium, provided the original work is properly cited.

sigma factors (σ^M, σ^W, σ^B), which ensure its induction under a broad variety of environmental stresses (12,13). Secondly, the cellular concentration of Spx is tightly maintained at a low level under reducing conditions by ClpXP-catalyzed proteolysis (14). Finally, the redox state of the cytoplasm is the major effector driving Spx activation. Under disulfide stress, the redox-sensitive CXXC motif of Spx undergoes a thiol–disulfide switch resulting in an oxidized Spx protein, which is the form reported to be efficient for transcriptional activation of the *trxA* and *trxB* promoters (15). Disulfide stress triggers the inactivation of both redox-sensitive PerR and YodB negative regulators of Spx (13,16). It also mediates the redox inactivation of the ClpX subunit, thus preventing the degradation of Spx by the ClpXP protease (14), and ensuring an immediate response to oxidative stress. These regulations result in increased *spx* transcription and in Spx accumulation in the cell.

Spx was reported to inhibit the transcription of some genes by preventing or disrupting the interaction of αCTD with the ComA and ResD activators (17,18). This anti-α activity was due to the increased Spx cellular concentration which interfered with the formation of the activator–αCTD RNAP–DNA complex and prevented transcription initiation (11,15). However, such a mechanism did not explain how Spx modulated specifically the transcription of genes independently of activators. Genetic and biochemical analyses performed with the *trxA* and *trxB* promoters provided evidence that a Spx–RNAP–DNA complex formed during Spx-mediated activation (15). The interaction of the Spx–RNAP–αCTD complex with the *trxB* promoter DNA required the *cis*-acting AGCA motif located upstream of the *trxB* core promoter sequences, suggesting that transcriptional activation in other Spx-controlled genes is also mediated by contacts between the Spx–RNAP complex with such *cis*-acting motifs (11,19).

Previous transcriptomic and proteomic studies have highlighted a large overlap in the genes differentially expressed under various stresses (12,20). In addition to Spx, several regulators are involved in the response to electrophilic compounds (16,21–24). Exposure of cells to diamide, different quinones and carbonyl electrophiles resulted in the induction of the CtsR, Spx and CymR regulons, indicating that these compounds inflict a common challenge to cellular thiol–redox homeostasis. The cross regulations between these effectors add another level of complexity to the stress responses. In this context, a global analysis of the genes differentially expressed when Spx interacts with RNAP revealed the key role of Spx in the regulation of thiol homeostasis but failed to discriminate between the genes directly and indirectly regulated by Spx (4).

Recently, the *B. subtilis* transcriptome was characterized under numerous environmental conditions, leading to the precise mapping of about 3000 promoters and transcription units (TUs) (25). As part of a systems biology approach to understand the global reorganization of the regulatory network during a nutrient shift, the DNA-binding sites of several TFs were identified before and after the shift and correlated with the genes differentially expressed under the same conditions. The results defined the genes under control of the TFs and helped refine our knowledge of the global *B. subtilis* regulatory network (26). Here, we used the above knowledge about promoters and a similar approach to identify the genes directly regulated by Spx under disulfide stress at the genomic scale. The chromosomal sites bound by the Spx–RNAP complex before and after a brief exposure of cells to sublethal diamide stress were mapped by chromatin immunopurification of a functional epitope-tagged Spx protein followed by hybridization of the captured DNA to tiling microarrays (ChIP–chip). In parallel, the genes differentially expressed in *spx*-proficient and -deficient strains exposed to the same stress conditions were identified. By combining Spx–RNAP-binding sites and differential expression of nearby genes, we identified 144 TUs under direct Spx control. Spx activation was validated by *in vitro* transcription analysis of selected promoters. The Spx-regulated promoters displayed an extended DNA motif located upstream of the −35 box for SigA recognition. We found that the nucleotide composition at some positions in the motif strongly correlated with Spx-mediated activation.

MATERIALS AND METHODS

Bacterial strains and growth conditions

All the strains and plasmids used in this study are listed in the Supplementary Data. *Bacillus subtilis* strains are derivatives of the BaSysBio reference strain BSB1 which is a tryptophan-prototrophic (*trp*+) obtained from the 168 strain (25). *Escherichia coli* MC1061 strain (27) was used for DNA manipulations. Bacterial cultures were performed at 37°C under vigorous shaking (240 rpm) in Luria Bertani (LB) rich medium supplemented with antibiotic when appropriate (5 μg/ml chloramphenicol, 0.6 μg/ml erythromycin, 100 μg/ml ampicillin) and IPTG (0.5 μg/ml). Diamide (Sigma-Aldrich) was added from a 100 mM stock solution into exponential growing cultures (OD_{600nm} of 0.6) to a final concentration of 0.5 mM. For RNA preparation, cells were harvested before ($t = 0$) and 5 min ($t = 5$) and 15 min ($t = 15$) after diamide addition. The sensitivity to diamide of the strains was measured by plating serial dilutions of stationary phase cultures on LB plates with and without 0.05 mM diamide and incubated overnight at 37°C.

A BSB1 strain expressing a C-terminal sequential peptide affinity (SPA)-tagged Spx protein (hereafter Spx^{SPA}) was constructed by chromosomal integration of a translational fusion between the *spx* coding sequence and the SPA tag sequence (28), resulting in the Bas044 strain expressing Spx^{SPA} under the control of its native promoter as unique source of Spx (see 'Supplementary Methods' section).

The *spx* mutant was constructed by homologous replacement of the Spx coding sequence with a chloramphenicol resistance gene (*cat*) using a joining PCR technique (see 'Supplementary Methods' section). The *spx* deletion mutant was obtained by transformation of the BSB1 strain with the joining PCR fragment and selection

for chloramphenicol resistance. Integration and deletion were confirmed by PCR and verified by DNA sequencing.

Genome-wide determination of the Spx-binding sites by ChIP–chip

Chromatin immunopurification of DNA bound by the protein complexes containing the SPA-tagged Spx was performed using the Bas044 strain as described (25). Briefly, exponentially growing cells were exposed or not to 0.5 mM diamide for 5 min, incubated with formaldehyde, the Spx^{SPA} was immune-precipitated and the DNA was purified (IP). The recovered DNA and the control whole-cell DNA extract (WCE) were labeled with Cy3 and Cy5, respectively, and cohybridized to the *B. subtilis* NimbleGen tiled microarrays as described (29) (see 'Supplementary Methods' section). Identification of peaks corresponding to chromosomal Spx-binding sites was performed as described (30). IP/WCE ratios ($\log_2$) were corrected for dye bias using Loess regression on the MA plot. The signal was smoothed by two rounds of sliding window (29 probes, ~320 bp) averaging. Maxima (or minima) positions were defined as probes for which the smoothed signal is the highest (or lowest respectively) into the window used for smoothing. Peaks within a same 300-bp window are merged. The peak height was calculated as the $\log_2$ ratio difference between the smoothed signal values at the maxima and the adjacent minima. In order to assess quantitatively the enrichment signal, the ChipScore was calculated as previously described (26). Briefly, this score is based on the distribution of the peak height values and estimates for each peak its distance from the median in units of the distance between the upper quartile and the median (ChipScore = [height-median]/[upperquartile-median]). Only the regions associated with a peak scoring > 4 [a threshold determined empirically from ChIP–chip experiments with TF CcpA (26)] in both replicates were considered as putative Spx-binding sites in the subsequent analyses. To reduce the number of putative non specific DNA-binding sites, the peaks repeatedly found in ChIP–chip experiments with other SPA-tagged proteins which were not associated with an effect on the expression of nearby genes in the Δ*spx* mutant or under diamide stress were not considered when defining the Spx regulon.

RNA preparation and transcriptome analysis

Total RNA was isolated as previously described (See 'Supplementary Methods' section). An aggregated expression value was computed for the genes annotated in the GenBank file AL009126.3 (31), and the newly defined transcribed regions (25). This value corresponds to the median of the smoothed signal (32) for probes lying entirely within the feature. Expression values were quantile-normalized between experiments (33). Differential expression analysis was performed using a Student's *t*-Test on $\log_2$ expression values of each gene to compare the wild-type (wt) strain and Δ*spx* mutant at $t = 0$ (before diamide addition) and by fitting a linear model to investigate the gene expression across the three time-points (0, 5 and 15 min) in the two strains (See 'Supplementary Methods' section). To avoid errors due to a potential saturation of the signal after induction by diamide stress, we examined all the genes with an expression level > 15.5 (at least at one time point) and found potential bias only for three TUs (*cysK*; *ctsR-mcsA-mcsB*; *clpE-S492*). These genes are marked by '(s)' in Supplementary Tables S3 and S5. The 44 broad functional categories defined by Kunst *et al.* (34) were extracted from SubtiList database (35).

Tandem-affinity purification of RNAP complexes

RNAP–protein complexes were purified as previously described (36) using a *B. subtilis* strain expressing a C-terminal SPA-tagged RpoB ($RpoB^{SPA}$) fusion protein. Briefly, 100 ml cultures were submitted to 0.5 mM diamide or not during 5 min, and $RpoB^{SPA}$ was purified sequentially using anti-FLAG antibody column followed by a calmodulin sepharose resin. Copurified proteins were identified by LC–MS/MS and their relative abundance was compared using the Protein Abundance Index (PAI) defined as the number of observed peptides divided by the number of observable peptides per protein (37).

Statistical analysis of the Spx-dependent promoter sequences

A statistical analysis of the DNA sequence surrounding the Spx-dependent transcriptional start sites (TSSs) detected by transcriptomics (see 'Results' section) was performed to map the −35 and −10 boxes. DNA sequences of length 101 bp (spanning from −60 bp to +40 bp) around the detected TSSs were extracted and bipartite motifs were searched with a preferential distance between the −10 box and the detected TSS using TREEMM, a new transdimensional RNAP-binding sites discovery algorithm (http://genome.jouy.inra.fr/~pnicolas/treemm/) (25). The relation between the occurrence of particular nucleotides at particular positions within the two boxes and the regulatory effect of Spx was investigated using ANOVA F-tests. The tests were performed separately for each of the 35 positions of the bipartite motif considered here (See 'Supplementary Methods' section). They consisted in determining whether the $\log_2$ expression ratio [Δ*spx* mutant versus wt] of the largest amplitude within the TU depended on the nucleotide found at that particular position.

Purification of *B. subtilis* Spx and RNA polymerase

Wt *spx* was amplified by PCR from the genomic DNA of *B. subtilis* 168, and cloned into an expression vector allowing in-frame fusion of a His_6 tag at the C-terminus of Spx. After transformation of *E. coli* GOLD strain, the expression of Spx-His_6 was induced with 1 mM IPTG for 3 h at 37°C. Cells were harvested, resuspended in 40 ml of buffer A containing 50 mM Tris–Cl pH 8, 1 M NaCl, lysed by sonication, and the cell lysate was centrifuged for 30 min at 20 000*g* at 4°C. The supernatant containing His-tagged Spx was loaded onto a Ni+ affinity column (Ni–NTA agarose, Qiagen). Spx-His_6 was eluted with imidazole, dialyzed against a buffer containing 50 mM Tris–Cl pH 8, 400 mM NaCl, 50% glycerol and stored

at −20°C. A His_6-tagged SpxC10A mutant protein was insoluble under the same conditions. *Bacillus subtilis* RNAP with a His_{10}-tagged β′ subunit was purified from the *spx*-null strain LK1119 (see 'Supplementary Methods' for strains description). The purification was done essentially as described (38) with the exception that no reducing agent was present during the purification process. The σ^A subunit of RNAP was overproduced from the pCD2 plasmid (39) and purified as described (40).

In vitro transcription assays

Eleven promoter regions covering approximately from −100 to +100 relative to the start of transcription were PCR amplified (see 'Supplementary Methods' for primer sequences), cloned via EcoRI and HindIII restriction sites into the p770 vector as previously described (41), and inserts of positive clones were resequenced. For *in vitro* transcription reactions, plasmid DNA was linearized with EcoRI, and the restriction enzyme was inactivated at 65°C for 15 min.

RNA polymerase isolated from LK1119 was reconstituted with saturating concentration of σ^A in storage buffer (50 mM Tris–HCl pH 8.0, 0.1 M NaCl, 50% glycerol) for 15 min at 37°C. Transcription assays were carried out essentially as described (15). Briefly, reactions were carried out in 10 µl: 30 nM holoenzyme ($RNAP\sigma^A$) was incubated for 30 min at 37°C with 1 nM linear DNA template in transcription buffer (40 mM Tris–HCl pH 8.0, 10 mM $MgCl_2$, 0.1 mg/ml BSA, 50 mM NaCl) in the presence or absence of Spx (10-fold molar excess over $RNAP\sigma^A$). Spx either was or was not pre-incubated with 5 mM DTT for 30 min at 37°C before addition to the transcription reaction. Reactions were started by NTPs (ATP, CTP and GTP were 200 µM; UTP was 10 µM plus 2 µM of radiolabeled [α-^{32}P]-UTP) and were allowed to proceed for 10 min at 37°C. Transcription reactions were terminated with equal volumes of formamide stop solution (95% formamide, 20 mM EDTA pH 8.0). Samples were loaded onto 7 M UREA 7 % polyacrylamide gels and electrophoresed. The dried gels were scanned with Molecular Imager_FX (BIO-RAD). The amounts of the transcripts (originating from the cloned promoters) were quantified with QuantityOne software (Biorad). All calculations and data fitting were done using SigmaPlot from Jandel Scientific.

RESULTS AND DISCUSSION

C-terminally SPA-tagged Spx is a fully functional regulator

In order to purify Spx from bacterial cells, the *B. subtilis* chromosome was modified at the *spx* locus to express Spx fused at its C-terminus with the SPA tag (Spx^{SPA}) (see 'Materials and Methods' section). In the resulting *spx-spa* strain, the Spx^{SPA} protein is under the control of its native expression signals and is the only source of Spx. The sensitivity to diamide of the *spx-spa* strain relative to the wt and *Δspx* deletion mutant strains was determined by measuring the efficiency of plating of stationary phase cultures on LB medium supplemented with 0.05 mM diamide. As previously reported the *Δspx* strain was highly sensitive to diamide (4). In contrast, the spx-*spa* strain exhibited a sensitivity similar to that of the wt strain (Figure 1A), indicating that Spx^{SPA} triggered the disulfide stress response as wt Spx. Disulfide stress is known to inhibit the ClpXP-catalyzed degradation of Spx thereby increasing Spx intracellular concentration (14). A western-blot analysis with anti-SPA antibodies revealed that Spx^{SPA} concentration increased in cells treated with diamide 0.5 mM (Figure 1B) whereas the *spx* mRNA abundance changed only slightly under this conditions (Figure 1C). These observations suggest that Spx^{SPA} is proteolysed in untreated cells. Exponentially growing cells ($OD_{600nm} = 0.6$) exposed to diamide (0.5 mM) displayed a similar transient growth arrest (~10 min) in the *spx-spa* and wt strains. In the *Δspx* mutant strain, growth recovery was slightly slower with a marginally reduced biomass produced (Figure 1D). From these results, we conclude that the Spx^{SPA} fusion protein is fully functional.

Genome-wide mapping of Spx-bound RNA polymerase-binding sites

In vitro, Spx binds to the C-terminal domain of the RNAP α subunit (4) but does not bind directly to DNA (11). To determine whether the Spx–RNAP complex occupies discrete DNA regions, we performed chromatin immunopurification of the DNA bound by the protein complexes containing the Spx^{SPA} protein. The *B. subtilis* strain expressing the functional Spx^{SPA} protein was treated or not with 0.5 mM diamide for 5 min, the protein–DNA complexes were crosslinked by formaldehyde and then immunoprecipitated. The significantly enriched DNA regions identified from the ChIP–chip signal (as described in 'Materials and Methods' section) correspond most likely to three-part complexes Spx–RNAP–DNA fixed by formaldehyde but can also include Spx in complex with yet unknown DNA-binding proteins and some non-specifically enriched DNA regions.

A total of 283 potential Spx–RNAP-binding sites were identified, 92 were present in both untreated and diamide-treated cells, 177 were specific of diamide-treated cells, and 14 were specific of untreated cells (Supplementary Table S1 and Supplementary Figures S1 and S2). A large majority of the sites (76%) was located within 150 bp of SigA TSS mapped previously (25), which is well above the expected 11% for peaks randomly distributed on the chromosome. This co-occurrence of Spx and SigA TSS fits well with our hypothesis that most of the peaks correspond to Spx–RNAP–DNA complexes. In addition, the Spx-containing complexes localize at defined DNA sites *in vivo* because most enriched DNA regions appeared as bell-shaped peaks (Figure 2), in sharp contrast with the extended enriched DNA regions observed after chromatin affinity precipitation of the *B. subtilis* RNAP core, which cover the promoter and most of the coding regions (42). These observations suggest that Spx associates with RNAP preferentially during transcription initiation and that the Spx–RNAP complex dissociates when transcription enters into

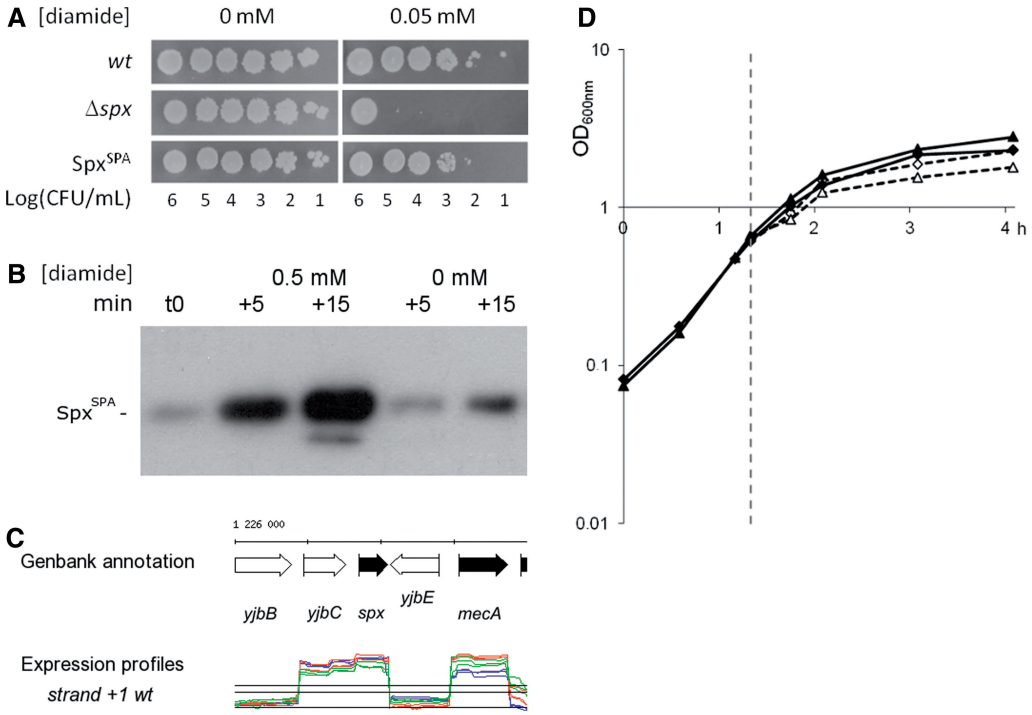

Figure 1. Phenotypes of *B. subtilis spx-spa* and Δ*spx* strains and Spx^{SPA} protein levels under diamide stress. (**A**) Diamide sensitivity of *B. subtilis* 168 *wt* strain, Δ*spx* mutant and strain carrying *spx-spa* translational fusion (Spx^{SPA}). Cells were grown aerobically in LB medium until stationary phase. Serial 10-fold dilutions were then plated on LB supplemented with 0.05 mM diamide (right) and no diamide (left). (**B**) Effect of diamide on Spx^{SPA} protein levels. Log-phase cultures of strain carrying *spx-spa* translational fusion were treated with 0.5 mM diamide or not. Cells were harvested before (t0) and 5 or 15 min after treatment and then disrupted by sonication. Total protein concentration was assayed with Bradford's method using BSA as control. SDS–PAGE was used to separate 3.5 µg of total proteins and Spx^{SPA} was revealed by western-blot using anti-M2 antibodies. A typical blot is shown. (**C**) Transcription profiles of the *spx* chromosome region (GenBank annotation) before (blue), 5 min (orange) and 15 min (green) after diamide addition, in triplicate (Supplementary Figure S1). (**D**) Typical growth curve of wt (diamond) and Δ*spx* mutant (triangle) strains treated with 0.5 mM diamide (dashed lines) or not (solid lines). Cells were grown aerobically in LB medium and diamide was added at OD_{600} = 0.6 (vertical dashed line). Under these conditions, the growth of the *spx-spa* strain is indistinguishable from wt.

the elongation phase. However, Spx–RNAP binding can sometimes extend into the CDS for some genes such as *trxB* (Figure 2), *ytsP* and *ypiA* (Supplementary Figure S1).

Spx is associated with RNA polymerase in both diamide stress and untreated conditions

The detection of putative Spx–RNAP-binding sites in cells not exposed to diamide is consistent with our previous observation that the Spx–RNAP protein complex could be detected by quantitative tandem affinity purification of RNAP in standard growth conditions (36). We used the same method to estimate the amount of RNAP associated with Spx in cells exposed to similar diamide stress conditions as in the ChIP–chip experiments. The RNAP protein complexes were purified using a *B. subtilis* strain expressing a C-terminal SPA-tagged RpoB fusion protein ($RpoB^{SPA}$) and the fractions of RNAP bound to selected proteins were determined as described in 'Materials and Methods' section. Whereas the fraction of RNAP bound to SigA changed only slightly with stress and represented ~60% of the purified RNAP complexes, the fraction of RNAP bound to Spx increased ~2-fold from 11% before stress to ~22% after diamide stress (Table 1). This result correlates with the observed increased number of Spx–RNAP-binding sites after diamide stress. Most Spx–RNAP-binding sites detected in untreated cells were common with those detected under diamide stress (92 out of 106), and the Spx–RNAP enrichment at these sites as measured by the ChIPscore (intended to normalize peak heights) tended to increase after stress (Figure 2 and Supplementary Table S1). Taken together, these findings strongly suggest that Spx–RNAP binds to promoter regions in absence of external oxidative stress, and that the number of DNA sites bound by Spx–RNAP and their occupancy increase with Spx concentration in the cell. Importantly, Spx–RNAP binding does not necessarily imply Spx-mediated transcriptional regulation because the redox state of cellular Spx, which is crucial for its regulatory activity (15), is unknown.

Transcriptional responses of *B. subtilis* exposed to a sublethal disulfide stress and role of Spx

Transcriptome analyses of the Δ*spx* mutant relative to wt were performed on cultures sampled at 0, 5 and 15 min after exposure to 0.5 mM diamide as described in 'Supplementary Methods' section. Transcripts were quantified according to our recently defined *B. subtilis* 168 structural annotation (25), which contains 1583 newly defined transcribed regions (nTRs) in addition to

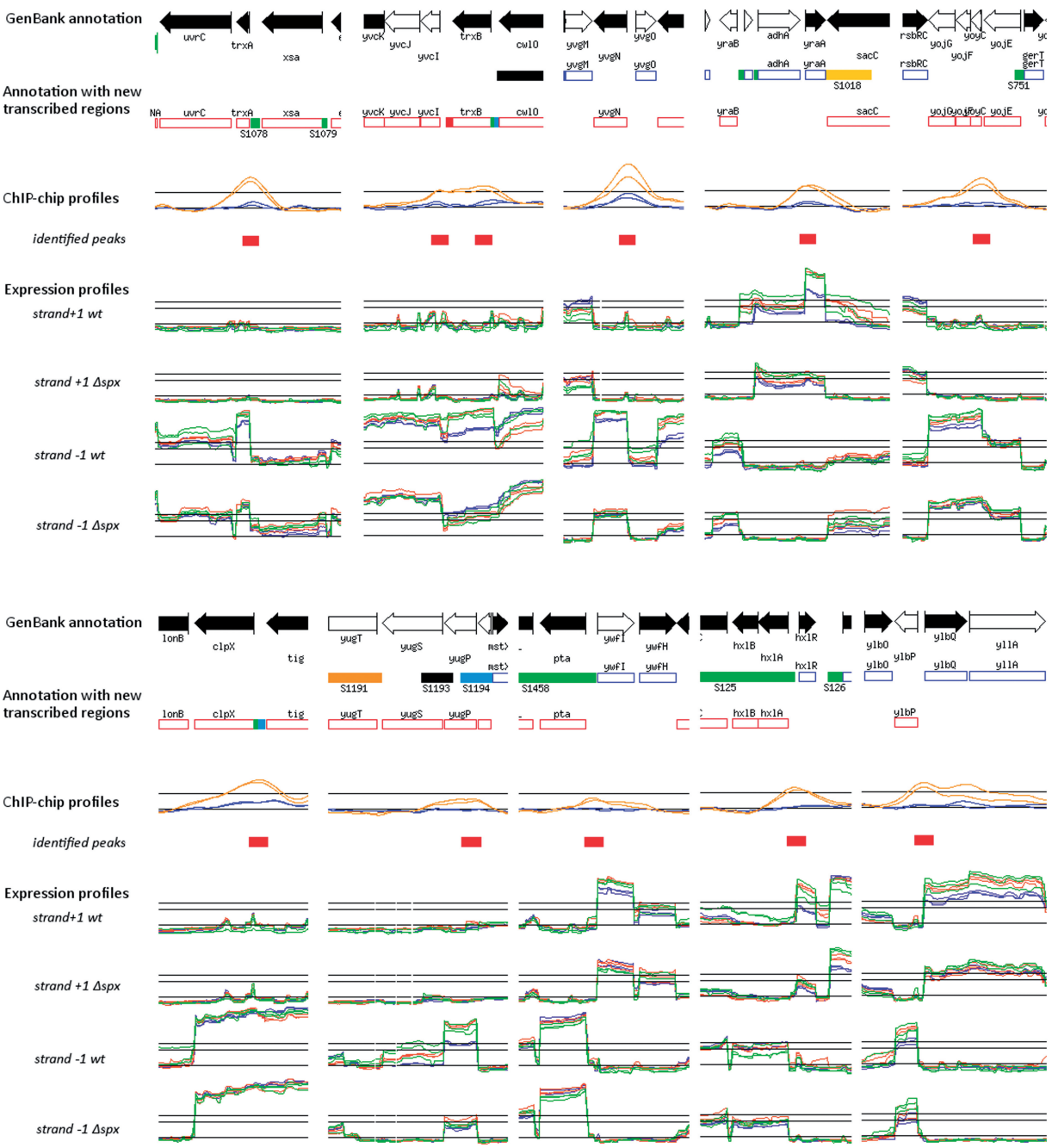

Figure 2. Typical Spx^{SPA}-RNAP-binding sites with corresponding expression profiles during diamide stress. Each of the 10 panels represents a chromosome region with annotations of CDSs and transcribed regions. The newly defined transcribed regions are indicated by colored boxes added to the predicted CDS (open boxes) as previously described (25): green, 5′; red, 3′-UTR; yellow, 3′-extended transcript after partial termination; black, new gene with own promoter and terminator. The ChIP–chip profiles from untreated (blue) and diamide-treated (orange) cells are in duplicate. Spx-binding sites corresponding to gene regulation are marked by red boxes. Expression profiles on the forward (+1) and reverse (−1) strands are shown for the *wt* and Δ*spx* mutant strains at t0 (blue), 5 min (orange) or 15 min (green) after diamide addition, in triplicate. The dataset for the complete genome can be visualized in the Supplementary Figure S1.

the 4292 previously annotated coding sequences (CDS) (Supplementary Table S2), and differentially expressed genes were identified (Supplementary Table S3). The exposure to a sublethal diamide stress of the wt strain entailed a global cellular response since 571 CDSs + 240 nTRs were upregulated and 732 CDSs + 211 nTRs were downregulated (Table 2 and Supplementary Figure S2). Among these differentially expressed transcripts, we found 194 genes previously reported to be induced after diamide stress (16), including several genes acting in oxidative stress resistance (*trxA*, *trxB*, *mrgA*, *perR*, *katA*) and the whole CtsR regulon, which is also induced by heat (43), by electrophiles (23,44) and by hypochlorite (45). We also found 229 genes previously reported to be

Table 1. Relative abundance of Spx in tandem-affinity purified RNAP complexes in cells treated or not with diamide

		No stress	Diamide stress
PAI	RpoA (35 kDa)	9.1	9.3
	SigA (43 kDa)	2.8	2.7
	Spx (15 kDa)	0.5	1.0
Relative fraction of RNAP bound to	SigA (%)	61.5	58.1
	Spx (%)	11	21.6

RNAP–protein complexes were purified using a *B. subtilis* strain expressing a C-terminal SPA-tagged RpoB fusion protein and copurified proteins were identified by mass spectrometry. The Protein Abundance Index (PAI), defined as the number of observed peptides divided by the number of observable peptides per protein (37), was used to estimate the relative abundance of Spx and SigA in the RNAP complexes. The stoichiometry of the RNAP ($2\alpha\beta\beta'$) was taken into account to calculate the Spx fraction relative to RpoA (α). This fraction might be overestimated due to the small number of peptides detected for Spx (36).

Table 2. Summary of transcribed regions (TRs) differentially expressed under diamide stress that are under potential Spx regulation

	Induction			Repression		
	No. of TRs	No. of CDSs	Ref.	No. of TRs	No. of CDSs	Ref.
Regulation by diamide	811	571	194[a]	943	732	229[a]
Regulation by Spx, total	570	424	74[b]	584	471	49[b]
Regulation by Spx, diamide induced	**408**	**298**	**68[b]**	68	57	0[b]
Regulation by Spx, diamide repressed	32	25	0[b]	**219**	**180**	**24[b]**

Previously defined TRs (1583 newly defined TRs and 4292 previously annotated CDS) (25), are considered differentially expressed with a $\log_2$-expression ratio of at least 1 (2-fold change on the linear scale) and a False-Discovery-Rate controlled at 5% (Supplementary Table S3). TRs were then grouped according to the sign of differential expression after diamide stress and in the *Δspx* mutant. For Spx-regulated (directly or indirectly) TRs, the sign of the regulation is taken at $t = 0$ (no diamide), and if no effect is observed at $t = 0$, it is taken at $t = 5$ and $t = 15$ (with diamide). The number of TRs corresponding to CDS is specified. The genes exhibiting impaired regulation in the *Δspx* mutant (boldfaced numbers) are considered as potentially regulated by Spx, either directly or indirectly. 'Ref.' column gives the number of those genes that have already been reported as regulated.
[a]by diamide stress (16)
[b]by the Spx–αCTD interaction (4).

repressed (16). The deletion of *spx* significantly impacted the expression of 1154 CDSs + nTRs of which 727 (63%) were common to the diamide response. In absence of Spx, the response to diamide was particularly affected since upregulation of 408 out of 811 CDSs + nTRs and downregulation of 219 out of 943 CDSs + nTRs were reduced. These genes are potentially under direct Spx control or might be indirectly regulated by Spx through pleiotropic effects (Table 2). The amplitude of the differential gene expression between wt and *Δspx* strains tended to increase between 5 and 15 min after diamide treatment, suggesting that the stress response was still ongoing.

Without stress, a much smaller number of transcripts were differentially expressed in the *Δspx* mutant (69 upregulated and 85 downregulated, Supplementary Table S3). Among them, several genes from the PBSX and SPβ prophages were detected, as previously observed in cells depleted of thioredoxin A (3) or in a *spx* mutant submitted to methylglyoxal stress (46). Interestingly, many of the genes downregulated in the Δ*spx* mutant under unstressed conditions encode proteins involved in resistance against oxidative stress (*trxA*, *nfrA*), detoxification (*mhqA*, *yraA*, *yvgN*, *pnbA*) and putative oxidoreductases (*yqiG*, *yqkF*, *ymaD, ykuU*), which are all strongly induced upon disulfide stress in the wt strain (Figure 2, see examples of *trxA* and *yvgN*). This suggests that Spx-mediated regulation (direct or indirect) is required for the basal expression of some redox homeostasis genes during normal growth.

The genes responsive to disulfide stress were grouped into previously defined functional categories (34). For each category, their proportion relative to the total number of genes in the category was analyzed and several categories exhibited a significant enrichment (Supplementary Table S4 and 'Supplementary Results' section). In particular, in the category 'RNA synthesis: regulation' which comprises 223 TFs, the mRNA abundance was changed upon disulfide stress for 80 TFs (including 29 TFs affected by the *spx* deletion), indicating a potentially large Spx indirect effect on transcriptional regulation. Our data also revealed many predicted small CDSs, small RNAs and antisense RNAs which could be potential players in the adaptive response to disulfide stress. Among the nTRs differentially expressed under diamide stress, 253 were regulated directly or indirectly by Spx (Supplementary Table S3, for details see 'Supplementary Results' section).

Definition of the Spx regulon

The genes under probable direct Spx control were defined by a combination of two criteria aimed at overcoming the limitations due to non-specific ChIP–chip signals and potentially large indirect transcriptomics effects. Namely, we searched for the simultaneous presence of (i) a potential Spx–RNAP-binding site overlapping the promoter region, and (ii) a statistically significant differential expression in the *Δspx* mutant relative to wt (with or without diamide stress). We found 127 Spx–RNAP-binding sites covering the promoter regions of 144 differentially expressed TUs (Supplementary Table S5). The 17 Spx–RNAP-binding sites mapping between divergently transcribed TUs likely corresponded to Spx–RNAP-binding sites in close proximity that could not be resolved by ChIP–chip. The group of 275 genes encompassed by these 144 TUs was defined as the probable Spx regulon for disulfide stress response. Of note, the two combined criteria lead to discard promoters bound by Spx–RNAP which are weakly or not differentially expressed in our conditions potentially because of the action of other regulators. For example, 67 Spx–RNAP-binding sites were located upstream of 70 TUs which exhibited no significant differential expression between the

Δspx and wt strains but were differentially expressed in the wt strain exposed to diamide stress. The 123 genes within this latter group were considered as putatively part of the Spx regulon (Supplementary Table S5). Finally, 89 Spx–RNAP-binding sites were not associated with any significant differential expression of neighboring genes in the *Δspx* mutant relative to wt and after diamide stress. These genes were not included in the Spx regulon.

Spx-regulated promoters display extended −10 and −35 boxes

To identify DNA sequence motifs specific of Spx regulated promoters, we analyzed the 144 TUs of the Spx regulon (Supplementary Table S5). The positions of the SigA-dependent transcription start sites (TSS) relative to these TUs were retrieved from our previous annotation of the transcriptome (25). When several TSSs were annotated, we carefully selected the one regulated by Spx based on the expression profiles of the *spx* mutant. A total of 131 unambiguous TSSs (103 positively- and 28 negatively-regulated promoters) were identified (Supplementary Table S6). Preliminary analyses with consensus-finding algorithms tailored for well conserved motifs (47) were not successful. Next, consensus bipartite SigA-binding motifs that could contain a Spx-binding signature were searched within the region of the TSSs. First, we processed separately the 103 TSSs positively regulated and the 28 negatively regulated promoters. This analysis revealed that Spx promoters do not share a unique consensus motif but rather exhibit extensions to the −35 and −10 boxes, suggesting that the combination of bases at several positions in these extensions determines the strength of Spx regulation. In particular, the consensus found for positively regulated promoters displayed an upstream extension of the −35 box not observed in negatively regulated promoters and in the two larger control sets (Supplementary Figure S3). However, these observations are not sufficient to conclude that the upstream-extended −35 box is absent in negatively regulated promoters because of the detection limits arising from the small number of promoters in this category.

To compare Spx-activated and repressed promoters more directly, we aligned simultaneously the 131 promoters to find a common consensus that was then searched for positions potentially predictive of the sign and strength of the regulation. The consensus, found in 120 out of the 131 TSSs, displayed extended −10 and −35 boxes, respectively composed of 19 and 16 bases including the aforementioned upstream-extension of the −35 box (Figure 3A). The −10 box TAtAAT and most of the −35 box TTGac (instead of TTGaca) were best conserved, and a motif TxTG (−17 to −14) as well as an A-rich extension downstream the −10 element exhibited some degree of sequence conservation. These elements are typical features of sigma(A) dependent promoters in *B. subtilis* (48). In contrast, the 11-nt extension upstream the −35 element did not display highly conserved positions (Figure 3A) but contained the positions −44 and −43 where nucleotides are best correlated with Spx transcriptional regulation (Figure 3B and Supplementary Table S6). We observed that G at position −44 and C at position −43 are strongly associated with Spx-mediated activation of the promoter and GC was the most frequent dinucleotide (71% of the promoters containing a C at position −43, Figure 3C). The occurrence of T at position −44 also led to Spx-dependent activation for most (22/25) promoters although the average activation level was somewhat lower than with G at −44 (Figure 3C). These findings are consistent with previous mutational analyses of the *trxA* and *trxB* promoters, which found the −45AGCA−42 *cis*-acting element to be required for Spx-dependent activation (11,19). However, the −45AGCA−42 element occurred only in 13 out of 131 Spx-dependent promoters suggesting that −45 and −42 positions are not critical for Spx regulation. These positions might still influence the magnitude of Spx regulation as the average transcriptional effect was strong for these 13 promoters (−3.08). From these findings we conclude that the base composition at position −43 appears the most important determinant for Spx-mediated activation. The extended elements in the core promoter are consistent with the model proposed for Spx-mediated transcriptional activation in which the Spx–RNAP α subunit complex interacts with these *cis*-acting elements and promotes Spx-induced initiation of transcription (11,15).

We observed that Spx-mediated repression was correlated with A at position −43 in the extended −35 element (Figure 3C). The presence of T at this position was also compatible with repression, and overall 21 out of 28 repressed promoters carried an A or T at position −43 (Supplementary Table S6). These observations raise the possibility that Spx may repress transcription by a mechanism involving its binding to RNAP at some promoters. The current model for Spx-mediated repression, which involves the negative interference by Spx of the interaction between a protein activator and RNAP (17,18), could also be compatible with the detection of Spx–RNAP-binding sites at repressed promoters if Spx interference takes place when RNAP is bound to the promoter. However, this hypothesis appears unlikely for the ComA-activated *srf* promoter, which is strongly repressed by Spx (4), since no Spx–RNAP binding was observed near *srf* (or any ComA-regulated gene). The Spx-repressed TUs (defined as overexpressed in *Δspx*) are generally also repressed after diamide treatment of wt cells, except for some TUs (*yceKJ*, *glpFK*, *yodB*, *katA*, *mrgA*) which encode functions of protection against oxidative killing (Supplementary Table S5). These observations suggest that Spx-mediated repression is potentially more complex than Spx-mediated activation, and will need future characterization.

Effect of Spx on *in vitro* transcription at newly identified promoters

To validate direct Spx activation on a subset of newly identified promoters, we performed *in vitro* transcription assays using purified Spx-free RNAP and purified Spx. The *trxB* and *rpsD* promoters were respectively used as positive and negative controls for Spx activation, as previously described (18,19). Because a Spx–RNAP-binding site was found near the *rpsD* promoter, we added two

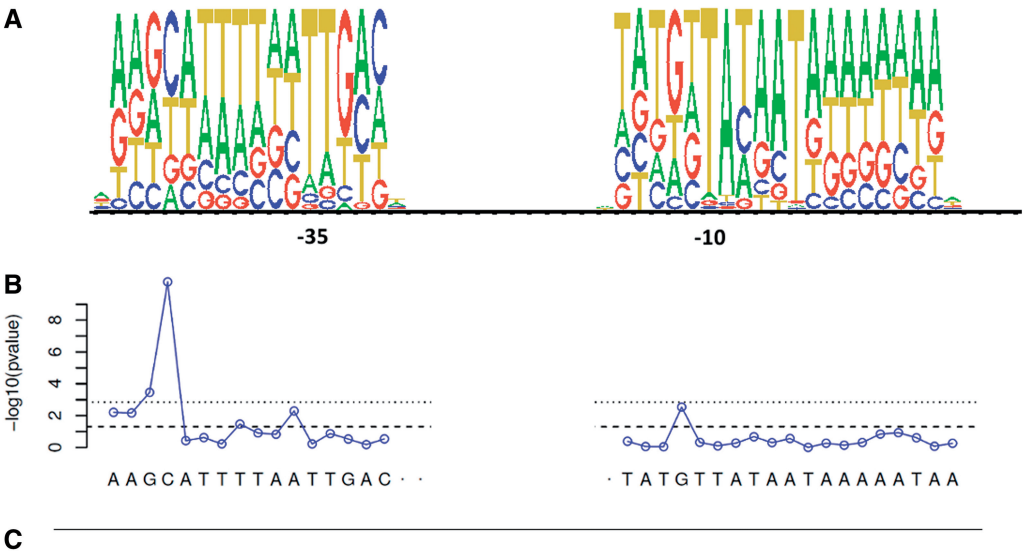

C

Log2 transcriptional ratio Δ*spx* versus *wt* in function of the nucleotidic composition

	-44 (n+/n-)	-43 (n+/n-)
A	-0.29 (20+/12-)	1.30 (3+/11-)
C	-0.34 (9+/6-)	-2.27 (51+/1-)
G	-1.95 (43+/5-)	-0.59 (12+/4-)
T	-1.35 (22+/3-)	-0.85 (28+/10-)
pvalue	*1.2E-02*	*1.4E-09*

Figure 3. Consensus DNA sequences of core promoters regulated by Spx. (**A**) Logo representation of the −35 and −10 consensus sequences derived from the 131 Spx-regulated promoters listed in Supplementary Table S6. (**B**) The probability of Spx-mediated transcriptional regulation associated with each nucleotide position within the −35 and −10 boxes was investigated using ANOVA F-tests. Spx regulation was estimated as the mean of the expression ratios (log_2) of maximal amplitude with the TUs in *Δspx* versus *wt*. The corresponding *P*-values are expressed as $-log_{10}$ for all positions. Horizontal lines correspond to a 0.05 threshold before (dashed line) and after (dotted line) the Bonferonni correction. (**C**) Correspondence between Spx regulation and nucleotide composition at the −44 and −43 positions. Spx transcriptional effect was estimated for each base at each position as (i) the average of maximal transcriptional ratios (as in B) and (ii) the occurrence of positive and negative regulations (n+/n−). *P*-values were adjusted for multiple-testing with Bonferroni correction (all data are available in Supplementary Table S6).

other promoters (*ycbG* and *yndB*) not regulated by Spx. Seven newly discovered Spx-regulated promoters were chosen to reflect a range of regulatory effects (from −1.28 for *clpX* to −3.45 for *yvgN*) and various levels of conservation of the previously described −45AGCA−42 *cis*-element (11) (from fully conserved in *yusI* promoter to only −43C in *ywfI* promoter, see details in Supplementary Table S6 and 'Supplementary Methods' section).

The *in vitro* transcription assays were conducted in the presence/absence of Spx, which was pre-incubated or not with DTT to reduce Spx (15). RNAP, purified from a *Δspx* strain, was devoid of Spx unless added. Transcription from the positive *trxB* promoter and from most of the newly identified promoters (Figure 4A and B) was strongly enhanced by oxidized Spx while the presence of DTT decreased the stimulatory effect. In contrast, transcription from promoters not regulated by Spx was only slightly affected by Spx (Figure 4C). An exception was P*yvgN* (Figure 4D) which displayed substantial stimulation by Spx irrespective of its redox state. Interestingly, the binding of Spx–RNAP at P*yvgN in vivo* was observed both with and without diamide stress (Figure 2). Taken together, these results confirm that the promoters newly identified by combined large-scale approaches are *bona fide* targets of Spx regulation.

Global biological role of the Spx regulon

The 144 TUs directly regulated by Spx comprise 275 genes among which 113 were previously reported to be affected by diamide (16) and 61 that were known to be affected by the disruption of Spx–αCTD interaction (4). Therefore, our study considerably expands the core Spx regulon by adding 101 genes and many novel transcribed regions including 5′-untranslated regions, small coding and non-coding RNA genes, and antisense RNAs (Supplementary Table S5 and 'Supplementary Results' section).

Cysteine and bacillithiol biosynthesis pathways are both controlled by Spx

In *B. subtilis*, both cysteine and bacillithiol act as redox buffers to maintain homeostasis during oxidative and thiol stresses. Recently *B. subtilis* was shown to synthesize the low-molecular-weight thiol bacillithiol, which is required for survival to several stresses including exposure to thiol-reactive compounds (49). Here, we report that

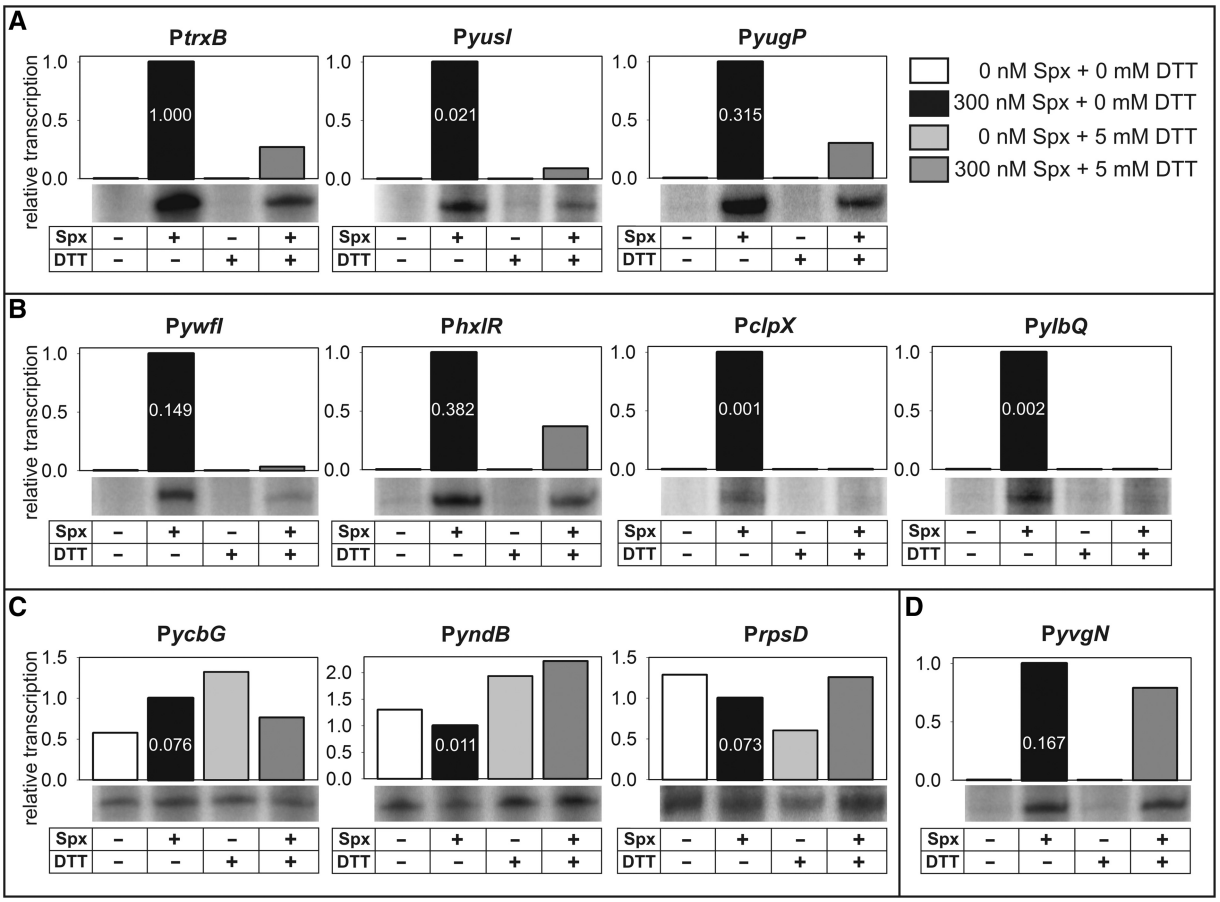

Figure 4. Effects of Spx on transcription *in vitro* from selected promoter regions. Transcription assays *in vitro* with *B. subtilis* RNAP in the presence/absence of Spx (10-fold molar excess over RNAP) and/or 5 mM DTT. For each promoter, representative data are shown, and transcription in the presence of oxidized Spx (without DTT) was set to 1 to aid in visualizing the effects. (**A**) Positive control promoter (P*trxB*) and two other promoters identified in our work to be stimulated by Spx. (**B**) Promoters selected from the newly identified promoters that are stimulated mainly by the oxidized form of Spx. (**C**) Negative control promoter (P*rpsD*) and two other promoters identified as not regulated by Spx. (**D**) P*yvgN*, a newly identified promoter that is stimulated both by oxidized and reduced Spx. The values of relative strength of the promoters (+Spx/-DTT) are indicated by white numbers over the corresponding black bars, and transcription is normalized to P*trxB* (set as 1). The differences in transcriptional activities *in vitro* spanned several orders of magnitude. Hence, to visualize transcription from all the promoters, the intensities of the primary data strips were adjusted individually for each promoter.

genes involved in cysteine and bacillithiol biosynthetic pathways are under direct Spx control (Supplementary Table S5). A Spx–RNAP-binding site was identified in the promoter regions of the *yrrT-mtnN-mccA-mccB-yrhC* operon, which encodes enzymes required for cysteine biosynthesis from methionine. Its induction was previously reported to occur in cells exposed to oxidative stress (16), and the transcriptional activation of the *yrrT* promoter by Spx was demonstrated *in vitro* (50). We showed that Spx highly represses *yezD,* which encodes a small uncharacterized protein also repressed by CymR (50), and that Spx activates the *tcyABC* operon encoding a L-cystine ABC transporter (51) not regulated by sulfate availability via CymR (52). With respect to bacillithiol, we found that the four biosynthesis genes were induced by diamide (Supplementary Table S3), with two of them, *bshB2* and *bshC,* under direct Spx regulation (Supplementary Table S5). The Spx-dependent induction of the promoter of the *ylbQ-bshC* TU was reproduced *in vitro* (Figure 4).

Spx is involved in the transcriptional regulation of other stress response regulons

The ClpP-dependent proteases control the stability of different regulators and they are key regulators of several adaptive responses. CtsR-regulated genes are induced by several stress conditions including heat (53), diamide (16) and hypochlorite stress (45). A molecular redox switch involving the McsA protein results in the inactivation of CtsR under oxidative stress (54). We found evidence that Spx acts also as a modulator of the proteolytic pathway because the three ATPases subunits of the Clp proteases (*clpX*, *clpE* and *clpC*), which are part of the CtsR regulon, were directly induced by Spx (Supplementary Table S5), and the *clpP* gene encoding the proteolytic subunit of Clp protease complex is putatively regulated by Spx (Spx–RNAP binding at the *clpP* promoter). Although the strong derepression caused by McsA-mediated inactivation of CtsR may be quantitatively more important than Spx regulation for the *ctsR* operon and *clpE* (Supplementary Table S5), the direct activation by Spx

was reproduced *in vitro* for the *clpX* promoter (Figure 4). The Spx-dependent induction of the Clp proteases likely contributes to rapidly eliminate misfolded proteins containing nonnative disulfide bonds resulting from the reaction of free thiol with diamide. YjbH promotes the ClpXP-catalyzed degradation of Spx (55,56). Interestingly, the *yjbI-yjbH-yizD* operon is directly activated by Spx (Supplementary Table S5). Since ClpX activity is impaired by oxidative stress, the Spx-dependent induction of both *yjbH* and *clpX* might correspond to a negative regulatory loop helping to maintain some ClpXP activity during stress, and facilitating the shutdown of the Spx-mediated response by reducing the cellular concentration of Spx. In addition, Spx directly regulates many uncharacterized proteins often predicted to be involved in maintaining the cell thiol redox status (Supplementary results).

Spx–RNAP-binding sites were identified at several promoters expressing TFs, suggesting that these TFs are directly controlled by Spx under diamide stress. Among them, *hxlR* and *yodB* encode electrophilic stress response regulators, and *yhdQ* (*cueR*) and *yceK* encode two putative transcriptional regulators shown to be induced by formaldehyde and methylglyoxal, respectively (23). Other putative TFs are induced in a Spx-dependent manner under diamide stress (*ydhJ*, *yczG*, *ykvZ* and *citR*) and some are repressed (*yerO*, *treR, yvoA* and *crh*). The direct regulation of these TFs by Spx suggests that they could act as secondary effectors in the global response to disulfide stress driven by Spx. Our results further document the interplay between Spx and other transcription regulators. For example, Spx directly regulates *mhqA* and *yodED*, which encode two dioxygenases/glyoxylases regulated by MhqR (22). Also, *yraA* involved in the degradation of thiol-containing proteins is under transcriptional control by both σ^B and AdhR (23) and is directly activated by Spx (Figure 2 and Supplementary Table S5). Finally, *katA* and *mrgA*, respectively encoding a catalase and an iron-storage protein, are both repressed by the peroxide stress regulator PerR and Spx–RNAP was bound to their promoters (Supplementary Table S5). The *spx* deletion results in an increased derepression of *katA* and *mrgA* genes (Supplementary Table S3) which is consistent to the previous expression data (17). The exact contribution of Spx to this regulation remains to be understood. In summary, Spx appears to be a global pleiotropic regulator which coregulates with several TFs, and perhaps coordinates, the more specific responses allowing the cell to cope with the various damages inflicted by disulfide stress.

Spx is required for the basal activity of some promoters in standard conditions

Spx was reported to activate transcription only under oxidizing conditions (15). Without diamide exposure, Spx is present at low concentration in the cell [Figure 1B, (15)] suggesting that the redox-sensitive ClpXP protease is active. Even though the redox status of Spx in cells is uncharacterized, Spx is expected to be mainly under its reduced form in these conditions. However, our study revealed that under standard growth conditions Spx–RNAP binding took place at 25% of the promoters for the 144 TUs directly regulated by Spx. We also found that Spx was required for the basal expression of 32 genes (Figure 2, see examples of *trxA* and *yvgN*; Supplementary Table S5). These results suggest that Spx activation can be mediated by the reduced form of Spx or that a fraction of Spx is oxidized even in the absence of external disulfide stress. The former possibility is consistent with our finding that the *in vitro* activation at P*yvgN* was comparable for the oxidized and reduced forms of Spx (Figure 4D). The interaction of Spx with RNAP αCTD was shown to be independent of the redox state of Spx (15). The ~2 fold increase of Spx–RNAP complexes observed under diamide stress is likely a consequence of Spx accumulation due to inactivation of ClpXP protease by oxidized conditions. The modulation of Spx amounts may act as an amplifier rather than as an on/off switch for the transcriptional stress response. Further studies will be required to understand how Spx redox state affects the DNA binding and the regulatory activity of Spx *in vivo*.

AVAILABILITY

All the raw data from this work have been deposited in GEO, and the following link has been created to allow review of record GSE35097: http://www.ncbi.nlm.nih.gov/geo/query/acc.cgi?token=xhszjiamusiymbg&acc=GSE35097

SUPPLEMENTARY DATA

Supplementary Data are available at NAR Online: Supplementary Tables 1–6, Supplementary Figures 1–3, Supplementary Methods, Supplementary Results and Supplementary References [57–67].

ACKNOWLEDGEMENTS

The authors are grateful to François Lecointe, Nathalie Pigeonneau, and Sandrine Auger for helpful methodological advices and insightful discussions, to M. Fogg and A. Wilkinson (University of York) for the Spx^{SPA} plasmid construction, to Alain Guillot (PAPSSO) for LC-MS/MS analyses, and to Isabelle Martin-Verstraete for helpful advices on sulfur pathways regulation and for providing BSY5000 strain. The authors thank our partners in the BaSysBio consortium for stimulating discussions.

FUNDING

European Commission-funded BaSysBio project [LSHG-CT-2006-037469]; Czech Science Foundation [P302/11/0855]; Institutional support [RVO:61388971]. Funding for open access charge: INRA.

Conflict of interest statement. None declared.

REFERENCES

1. Mostertz,J., Hochgrafe,F., Jurgen,B., Schweder,T. and Hecker,M. (2008) The role of thioredoxin TrxA in *Bacillus subtilis*: a proteomics and transcriptomics approach. *Proteomics*, **8**, 2676–2690.
2. Scharf,C., Riethdorf,S., Ernst,H., Engelmann,S., Volker,U. and Hecker,M. (1998) Thioredoxin is an essential protein induced by multiple stresses in *Bacillus subtilis*. *J. Bacteriol.*, **180**, 1869–1877.
3. Smits,W.K., Dubois,J.Y., Bron,S., van Dijl,J.M. and Kuipers,O.P. (2005) Tricksy business: transcriptome analysis reveals the involvement of thioredoxin A in redox homeostasis, oxidative stress, sulfur metabolism, and cellular differentiation in *Bacillus subtilis*. *J. Bacteriol.*, **187**, 3921–3930.
4. Nakano,S., Kuster-Schock,E., Grossman,A.D. and Zuber,P. (2003) Spx-dependent global transcriptional control is induced by thiol-specific oxidative stress in *Bacillus subtilis*. *Proc. Natl Acad. Sci. USA*, **100**, 13603–13608.
5. Duwat,P., Ehrlich,S.D. and Gruss,A. (1999) Effects of metabolic flux on stress response pathways in *Lactococcus lactis*. *Mol. Microbiol.*, **31**, 845–858.
6. Wang,C., Fan,J., Niu,C., Wang,C., Villaruz,A.E., Otto,M. and Gao,Q. (2010) Role of *spx* in biofilm formation of *Staphylococcus epidermidis*. *FEMS Immunol. Med. Microbiol.*, **59**, 152–160.
7. Kajfasz,J.K., Rivera-Ramos,I., Abranches,J., Martinez,A.R., Rosalen,P.L., Derr,A.M., Quivey,R.G. and Lemos,J.A. (2010) Two Spx proteins modulate stress tolerance, survival, and virulence in *Streptococcus mutans*. *J. Bacteriol.*, **192**, 2546–2556.
8. Turlan,C., Prudhomme,M., Fichant,G., Martin,B. and Gutierrez,C. (2009) SpxA1, a novel transcriptional regulator involved in X-state (competence) development in *Streptococcus pneumoniae*. *Mol. Microbiol.*, **73**, 492–506.
9. Pamp,S.J., Frees,D., Engelmann,S., Hecker,M. and Ingmer,H. (2006) Spx is a global effector impacting stress tolerance and biofilm formation in *Staphylococcus aureus*. *J. Bacteriol.*, **188**, 4861–4870.
10. Reder,A., Hoper,D., Weinberg,C., Gerth,U., Fraunholz,M. and Hecker,M. (2008) The Spx paralogue MgsR (YqgZ) controls a subregulon within the general stress response of *Bacillus subtilis*. *Mol. Microbiol.*, **69**, 1104–1120.
11. Reyes,D.Y. and Zuber,P. (2008) Activation of transcription initiation by Spx: formation of transcription complex and identification of a Cis-acting element required for transcriptional activation. *Mol. Microbiol.*, **69**, 765–779.
12. Antelmann,H., Scharf,C. and Hecker,M. (2000) Phosphate starvation-inducible proteins of *Bacillus subtilis*: proteomics and transcriptional analysis. *J. Bacteriol.*, **182**, 4478–4490.
13. Leelakriangsak,M., Kobayashi,K. and Zuber,P. (2007) Dual negative control of *spx* transcription initiation from the P3 promoter by repressors PerR and YodB in *Bacillus subtilis*. *J. Bacteriol.*, **189**, 1736–1744.
14. Zhang,Y. and Zuber,P. (2007) Requirement of the zinc-binding domain of ClpX for Spx proteolysis in *Bacillus subtilis* and effects of disulfide stress on ClpXP activity. *J. Bacteriol.*, **189**, 7669–7680.
15. Nakano,S., Erwin,K.N., Ralle,M. and Zuber,P. (2005) Redox-sensitive transcriptional control by a thiol/disulphide switch in the global regulator, Spx. *Mol. Microbiol.*, **55**, 498–510.
16. Leichert,L.I., Scharf,C. and Hecker,M. (2003) Global characterization of disulfide stress in *Bacillus subtilis*. *J. Bacteriol.*, **185**, 1967–1975.
17. Nakano,S., Nakano,M.M., Zhang,Y., Leelakriangsak,M. and Zuber,P. (2003) A regulatory protein that interferes with activator-stimulated transcription in bacteria. *Proc. Natl Acad. Sci. USA*, **100**, 4233–4238.
18. Zhang,Y., Nakano,S., Choi,S.Y. and Zuber,P. (2006) Mutational analysis of the *Bacillus subtilis* RNA polymerase alpha C-terminal domain supports the interference model of Spx-dependent repression. *J. Bacteriol.*, **188**, 4300–4311.
19. Nakano,M.M., Lin,A., Zuber,C.S., Newberry,K.J., Brennan,R.G. and Zuber,P. (2010) Promoter recognition by a complex of Spx and the C-terminal domain of the RNA polymerase alpha subunit. *PLoS One*, **5**, e8664.
20. Tam le,T., Antelmann,H., Eymann,C., Albrecht,D., Bernhardt,J. and Hecker,M. (2006) Proteome signatures for stress and starvation in *Bacillus subtilis* as revealed by a 2-D gel image color coding approach. *Proteomics*, **6**, 4565–4585.
21. Leelakriangsak,M., Huyen,N.T., Towe,S., van Duy,N., Becher,D., Hecker,M., Antelmann,H. and Zuber,P. (2008) Regulation of quinone detoxification by the thiol stress sensing DUF24/MarR-like repressor, YodB in *Bacillus subtilis*. *Mol. Microbiol.*, **67**, 1108–1124.
22. Towe,S., Leelakriangsak,M., Kobayashi,K., Van Duy,N., Hecker,M., Zuber,P. and Antelmann,H. (2007) The MarR-type repressor MhqR (YkvE) regulates multiple dioxygenases/glyoxalases and an azoreductase which confer resistance to 2-methylhydroquinone and catechol in *Bacillus subtilis*. *Mol. Microbiol.*, **66**, 40–54.
23. Nguyen,T.T., Eiamphungporn,W., Mader,U., Liebeke,M., Lalk,M., Hecker,M., Helmann,J.D. and Antelmann,H. (2009) Genome-wide responses to carbonyl electrophiles in *Bacillus subtilis*: control of the thiol-dependent formaldehyde dehydrogenase AdhA and cysteine proteinase YraA by the MerR-family regulator YraB (AdhR). *Mol. Microbiol.*, **71**, 876–894.
24. Yurimoto,H., Hirai,R., Matsuno,N., Yasueda,H., Kato,N. and Sakai,Y. (2005) HxlR, a member of the DUF24 protein family, is a DNA-binding protein that acts as a positive regulator of the formaldehyde-inducible *hxlAB* operon in *Bacillus subtilis*. *Mol. Microbiol.*, **57**, 511–519.
25. Nicolas,P., Mäder,U., Dervyn,E., Rochat,T., Leduc,A., Pigeonneau,N., Bidnenko,E., Marchadier,E., Hoebeke,M., Aymerich,S. *et al.* (2012) Condition-dependent transcriptome reveals high-level regulatory architecture in *Bacillus subtilis*. *Science*, **335**, 1103–1106.
26. Buescher,J.M., Liebermeister,W., Jules,M., Uhr,M., Muntel,J., Botella,E., Hessling,B., Kleijn,R.J., Le Chat,L., Lecointe,F. *et al.* (2012) Global network reorganization during dynamic adaptations of *Bacillus subtilis* metabolism. *Science*, **335**, 1099–1103.
27. Casadaban,M.J. and Cohen,S.N. (1980) Analysis of gene control signals by DNA fusion and cloning in *Escherichia coli*. *J. Mol. Biol.*, **138**, 179–207.
28. Zeghouf,M., Li,J., Butland,G., Borkowska,A., Canadien,V., Richards,D., Beattie,B., Emili,A. and Greenblatt,J.F. (2004) Sequential Peptide Affinity (SPA) system for the identification of mammalian and bacterial protein complexes. *J. Proteome Res.*, **3**, 463–468.
29. Rasmussen,S., Nielsen,H.B. and Jarmer,H. (2009) The transcriptionally active regions in the genome of *Bacillus subtilis*. *Mol. Microbiol.*, **73**, 1043–1057.
30. Reppas,N.B., Wade,J.T., Church,G.M. and Struhl,K. (2006) The transition between transcriptional initiation and elongation in *E. coli* is highly variable and often rate limiting. *Mol. Cell*, **24**, 747–757.
31. Barbe,V., Cruveiller,S., Kunst,F., Lenoble,P., Meurice,G., Sekowska,A., Vallenet,D., Wang,T., Moszer,I., Medigue,C. *et al.* (2009) From a consortium sequence to a unified sequence: the *Bacillus subtilis* 168 reference genome a decade later. *Microbiology*, **155**, 1758–1775.
32. Nicolas,P., Leduc,A., Robin,S., Rasmussen,S., Jarmer,H. and Bessieres,P. (2009) Transcriptional landscape estimation from tiling array data using a model of signal shift and drift. *Bioinformatics*, **25**, 2341–2347.
33. Bolstad,B.M., Irizarry,R.A., Astrand,M. and Speed,T.P. (2003) A comparison of normalization methods for high density oligonucleotide array data based on variance and bias. *Bioinformatics*, **19**, 185–193.
34. Kunst,F., Ogasawara,N., Moszer,I., Albertini,A.M., Alloni,G., Azevedo,V., Bertero,M.G., Bessieres,P., Bolotin,A., Borchert,S. *et al.* (1997) The complete genome sequence of the gram-positive bacterium *Bacillus subtilis*. *Nature*, **390**, 249–256.
35. Moszer,I., Jones,L.M., Moreira,S., Fabry,C. and Danchin,A. (2002) SubtiList: the reference database for the *Bacillus subtilis* genome. *Nucleic Acids Res.*, **30**, 62–65.
36. Delumeau,O., Lecointe,F., Muntel,J., Guillot,A., Guedon,E., Monnet,V., Hecker,M., Becher,D., Polard,P. and Noirot,P. (2011)

The dynamic protein partnership of RNA polymerase in *Bacillus subtilis*. *Proteomics*, **11**, 2992–3001.
37. Ishihama,Y., Oda,Y., Tabata,T., Sato,T., Nagasu,T., Rappsilber,J. and Mann,M. (2005) Exponentially modified protein abundance index (emPAI) for estimation of absolute protein amount in proteomics by the number of sequenced peptides per protein. *Mol. Cell. Proteomics*, **4**, 1265–1272.
38. Qi,Y. and Hulett,F.M. (1998) PhoP-P and RNA polymerase sigmaA holoenzyme are sufficient for transcription of Pho regulon promoters in *Bacillus subtilis*: PhoP-P activator sites within the coding region stimulate transcription *in vitro*. *Mol. Microbiol.*, **28**, 1187–1197.
39. Chang,B.Y. and Doi,R.H. (1990) Overproduction, purification, and characterization of *Bacillus subtilis* RNA polymerase sigma A factor. *J. Bacteriol.*, **172**, 3257–3263.
40. Juang,Y.L. and Helmann,J.D. (1994) A promoter melting region in the primary sigma factor of *Bacillus subtilis*. Identification of functionally important aromatic amino acids. *J. Mol. Biol.*, **235**, 1470–1488.
41. Sojka,L., Kouba,T., Barvik,I., Sanderova,H., Maderova,Z., Jonak,J. and Krasny,L. (2011) Rapid changes in gene expression: DNA determinants of promoter regulation by the concentration of the transcription initiating NTP in *Bacillus subtilis*. *Nucleic Acids Res.*, **39**, 4598–4611.
42. Ishikawa,S., Oshima,T., Kurokawa,K., Kusuya,Y. and Ogasawara,N. (2010) RNA polymerase trafficking in *Bacillus subtilis* cells. *J. Bacteriol.*, **192**, 5778–5787.
43. Kruger,E., Witt,E., Ohlmeier,S., Hanschke,R. and Hecker,M. (2000) The clp proteases of *Bacillus subtilis* are directly involved in degradation of misfolded proteins. *J. Bacteriol.*, **182**, 3259–3265.
44. Antelmann,H., Hecker,M. and Zuber,P. (2008) Proteomic signatures uncover thiol-specific electrophile resistance mechanisms in *Bacillus subtilis*. *Expert Rev. Proteomics*, **5**, 77–90.
45. Chi,B.K., Gronau,K., Mader,U., Hessling,B., Becher,D. and Antelmann,H. (2011) S-bacillithiolation protects against hypochlorite stress in *Bacillus subtilis* as revealed by transcriptomics and redox proteomics. *Mol. Cell. Proteomics*, **10**, M111 009506.
46. Zuber,P., Chauhan,S., Pilaka,P., Nakano,M.M., Gurumoorthy,S., Lin,A.A., Barendt,S.M., Chi,B.K., Antelmann,H. and Mader,U. (2011) Phenotype enhancement screen of a regulatory *spx* mutant unveils a role for the *ytpQ* gene in the control of iron homeostasis. *PLoS One*, **6**, e25066.
47. Bailey,T.L., Boden,M., Buske,F.A., Frith,M., Grant,C.E., Clementi,L., Ren,J., Li,W.W. and Noble,W.S. (2009) MEME SUITE: tools for motif discovery and searching. *Nucleic Acids Res.*, **37**, W202–W208.
48. Helmann,J.D. (1995) Compilation and analysis of *Bacillus subtilis* sigma A-dependent promoter sequences: evidence for extended contact between RNA polymerase and upstream promoter DNA. *Nucleic Acids Res.*, **23**, 2351–2360.
49. Gaballa,A., Newton,G.L., Antelmann,H., Parsonage,D., Upton,H., Rawat,M., Claiborne,A., Fahey,R.C. and Helmann,J.D. (2010) Biosynthesis and functions of bacillithiol, a major low-molecular-weight thiol in *Bacilli*. *Proc. Natl Acad. Sci. USA*, **107**, 6482–6486.
50. Choi,S.Y., Reyes,D., Leelakriangsak,M. and Zuber,P. (2006) The global regulator Spx functions in the control of organosulfur metabolism in *Bacillus subtilis*. *J. Bacteriol.*, **188**, 5741–5751.
51. Burguiere,P., Auger,S., Hullo,M.F., Danchin,A. and Martin-Verstraete,I. (2004) Three different systems participate in L-cystine uptake in *Bacillus subtilis*. *J. Bacteriol.*, **186**, 4875–4884.
52. Even,S., Burguiere,P., Auger,S., Soutourina,O., Danchin,A. and Martin-Verstraete,I. (2006) Global control of cysteine metabolism by CymR in *Bacillus subtilis*. *J. Bacteriol.*, **188**, 2184–2197.
53. Kruger,E., Volker,U. and Hecker,M. (1994) Stress induction of *clpC* in *Bacillus subtilis* and its involvement in stress tolerance. *J. Bacteriol.*, **176**, 3360–3367.
54. Elsholz,A.K., Hempel,K., Pother,D.C., Becher,D., Hecker,M. and Gerth,U. (2011) CtsR inactivation during thiol-specific stress in low GC, Gram+ bacteria. *Mol. Microbiol.*, **79**, 772–785.
55. Garg,S.K., Kommineni,S., Henslee,L., Zhang,Y. and Zuber,P. (2009) The YjbH protein of *Bacillus subtilis* enhances ClpXP-catalyzed proteolysis of Spx. *J. Bacteriol.*, **191**, 1268–1277.
56. Larsson,J.T., Rogstam,A. and von Wachenfeldt,C. (2007) YjbH is a novel negative effector of the disulphide stress regulator, Spx, in *Bacillus subtilis*. *Mol. Microbiol.*, **66**, 669–684.